Journal of Controlled Release 394 (2026) 114861

Contents lists available at ScienceDirect

Journal of Controlled Release

journal homepage: www.elsevier.com/locate/jconrel

Hyaluronan and gellan nanohydrogels exhibit an unexpected activity in hampering *Staphylococcus epidermidis* biofilm☆

Anna Pietrella [a], Irene Paris [b], Claudia Migliorini [a], Marco Morelli [c], Andrea Carpentieri [c], Pietro Matricardi [a,d,*], Chiara Di Meo [a,1], Rosanna Papa [b,1]

[a] Department of Drug Chemistry and Technologies, Sapienza University of Rome, Piazzale Aldo Moro 5, 00185 Rome, Italy.
[b] Department of Public Health and Infectious Diseases, Sapienza University of Rome, Piazzale Aldo Moro 5, 00185 Rome, Italy.
[c] Department of Chemical Sciences, University of Naples Federico II, Strada Comunale Cinthia 26, 80126 Naples, Italy.
[d] Department of Biology, Tor Vergata University of Rome, Via della Ricerca Scientifica 1, 00133 Rome, Italy

ARTICLE INFO

Keywords:
Nanohydrogels
Staphylococcus epidermidis
Anti-biofilm
Polysaccharides
Hyaluronic acid
Gellan gum

ABSTRACT

In clinical settings, the intensive use of antibiotics, particularly in intensive care settings, leads to a significant increase in the number of bacterial species that are resistant to treatments. In this context, biofilm is a crucial virulence factor that enable bacteria to persist within the host, often resulting in the need for extensive antibiotic treatment. *Staphylococcus epidermidis*, a notable nosocomial pathogen, poses a risk to vulnerable patients due to its ability to form biofilms on indwelling medical devices and its high resistance to antibiotic therapy. For this purpose, investigating alternative strategies that target the virulence of pathogens could offer a promising alternative strategy. In this study, we analyzed innovative polymeric materials, such as polysaccharide-based nanohydrogels, for their potential application contrasting *S. epidermidis* monospecies biofilm on the surfaces of materials most employed in medical devices. These nanohydrogels were found to be effective in eradicating the biofilm matrix and preventing bacterial adhesion. Additionally, the treatment with hyaluronan-based nanohydrogels altered the surface protein profile of *S. epidermidis*, leading to the disappearance of AtlE, the primary autolysin involved in biofilm formation, suggesting a potential mechanism of action for these nanogels. Data are available via ProteomeXchange with identifier PXD074516.

1. Introduction

Staphylococcus epidermidis (*S. epidermidis*) is an opportunistic pathogen that is part of our cutaneous microbiome, primarily implicated in healthcare-associated infections, particularly those related to implanted medical devices [2,6]. These infections encompass endocarditis of prosthetic valves, intravascular catheter infections, joint replacements, and orthopedic implants, as well as sepsis in premature infants, urinary tract infections, and surgical wound infections. Among these medical device-associated infections, mono-species infections - most frequently caused by *S. epidermidis* - constitute the predominant form encountered in clinical practice [29,40]. The eradication of this pathogen poses significant challenges due to its ability to form biofilm, a key virulence factor. Through biofilm formation, the bacterium can persist in structured microbial communities and becomes resilient to conventional antimicrobial therapies [15,29]. Biofilm can develop on a variety of biotic and abiotic surfaces [19], with bacteria encased in a self-produced extracellular matrix mainly composed by polysaccharides, extracellular DNA (eDNA) and proteins. The structure of the biofilm provides mechanical and structural stability for the bacteria, while also acting as a chemical and physical barrier. The small pores and channels within the biofilm make it particularly difficult for molecules to penetrate, resulting in significantly greater antibiotic tolerance compared to bacteria in their planktonic growth. While increasing dosages of antibiotics may allow more of the drug to reach the bacteria within the matrix, this approach simultaneously heightens the risk of drug toxicity and the development of antimicrobial resistance [8,39].

This situation highlights the urgent need for alternative therapies to combat pathogens that no longer respond to traditional medications. One promising strategy is to focus on disrupting bacterial virulence

☆ This article is part of a Special issue entitled: 'Hydrogels in Medicine' published in Journal of Controlled Release.

* Corresponding author at: Department of Biology, Tor Vergata University of Rome, Via della Ricerca Scientifica 1, 00133 Rome, Italy.
E-mail address: pietro.matricardi@uniroma2.it (P. Matricardi).

[1] These authors equally contributed to the work.

https://doi.org/10.1016/j.jconrel.2026.114861
Received 23 November 2025; Received in revised form 6 March 2026; Accepted 22 March 2026
Available online 23 March 2026

factors instead of relying solely on bactericidal agents, as this approach may help prevent the rapid emergence of resistant mutants [31]. In this context, numerous studies have demonstrated the effectiveness and potential of nanotechnology in treating diseases associated with biofilms. These advanced systems can deliver therapeutic agents directly to the biofilm, effectively targeting its structures and facilitating penetration into the matrix [1,20,21,45].

Among nanosystems, a versatile class is represented by nanohydrogels (NHs). They are aqueous dispersions of polymer chains that are interconnected by physical or chemical bonds, forming a complex network at the nanometer scale. The polymer chains can be engineered to spontaneously trap hydrophilic or lipophilic drugs through the formation of ionic bonds, salt bridges, or hydrophobic interactions. Additionally, these nanohydrogels are highly stable, can load significant amounts of drugs, and can modify their properties in response to environmental stimuli such as pH and temperature. These characteristics make them promising candidates for drug delivery systems. In addition to the advantages of NHs, the ones that present natural polymers as main constituent (e.g. polysaccharides) are biocompatible, biodegradable and nontoxic. When derivatized with cholesterol, polymer chains of polysaccharides, hyaluronic acid (HA) and gellan (Ge), form amphiphilic compounds designated as HA-CH and Ge-CH. These compounds can then be used to synthesize NHs through a self-assembly technique. The potential of these specific NHs as drug delivery systems has been studied and discussed in previous literature [3,12,22,23,25–27,42,43,48]. However, despite numerous reports on their delivery capabilities, a deep focus on the possibility to affect biofilm, related to the intrinsic characteristic of their main constituents rather than the active molecule they deliver, has not yet been investigated.

In this project, we investigated the anti-adhesive and anti-biofilm efficacy of HA-CH and Ge-CH nanohydrogels on two *S. epidermidis* strains obtained from the American Type Culture Collection (ATCC). Surprisingly, the results revealed a strong effect of HA-CH and Ge-CH on bacterial adhesion and biofilm, only when they were formulated as nanogels.

2. Materials and methods

2.1. Materials

Sodium hyaluronan (HA, $M_W = 2.20 \times 10^5$ according to the supplier) was purchased from Contipro (Dolni Dobrouč, Czech Republic), Gellan gum (Ge, $M_w = 2.5 \times 10^6$ according to the supplier) was a Kelko product and was purchased from Giusto Faravelli (Milan, Italy). The polymers were then exchanged in tetrabutylammonium salts (HA^-TBA^+ and Ge^-TBA^+) by using a Dowex resin. Cholesterol (CH), 4-bromobutyrric acid (CH-Br), *N*-Methyl-2-pyrrolidone (NMP), *N*-(3-dimethylaminopropyl)-*N*′-(ethylcarbodimide hydrochloride) (EDC•HCl), 4-(Dimethyl amino) pyridine (DMAP), Phosphate Buffered Saline (PBS) and *Micrococcus luteus* were Sigma-Aldrich products and were purchased from Merck Life Science, Milan, Italy. Brain Heart Infusion Broth (BHI) and Tryptone Soya Broth (TSB) were purchased from Oxoid, Basingstoke, UK. Agarose was purchased from Invitrogen, Paisley, UK. Coomassie Brilliant Blue and 30% Acrylamide/Bis Solution 29:1 was purchased from Bio-Rad, Milan, Italy. mPAGE Color Protein Standard was purchased from Millipore, Milan, Italy. 250 blue restained marker was purchased from Vazyme, Nanjing, PRC. LTQ Orbitrap XL Hybrid Ion Trap-Orbitrap MS System was purchased from Thermo Scientific, Bremen, Germany.

2.2. Bacterial strains and culture conditions

S. epidermidis strains used in this research are major biofilm producers and belong to the American Type Culture Collection (ATCC). *S. epidermidis* O47 was isolated in 1996 by a patient with an infection caused by an orthopedic implant [35]; *S. epidermidis* RP62A strain was extracted between 1979 and 1980 by patients involved in an epidemic sepsis, associated with intravascular catheters [41]. The bacteria, stored in frozen glycerol stock at −80 °C, were streaked on solid TSA plates and incubated for 24 h at 37 °C. To provide fresh colonies as needed, a single colony was sub-cultured in 10 mL of BHI under vigorous agitation (180 rpm) for 24 h at 37 °C.

2.3. HA-CH and Ge-CH NHs preparation

HA-CH and Ge-CH derivatives were synthesized as previously described in earlier studies [12,25,26]. In brief, 500 mg (1.3 mmol) of CH was reacted with 648 mg (0.9 mmol) of 4-bromo-butyric acid, 744 mg (3.9 mmol) of EDC•HCl, and 79 mg (0.65 mmol) of DMAP in 10 mL of CH_2Cl_2 overnight at room temperature. The resulting product was purified using a silica column with a mixture of cyclohexane and ethyl acetate (in a 99:1 ratio), yielding approximately 500 mg of CH-Br. Next, 200 mg of HA^-TBA^+ and 34.3 mg of CH-Br were dissolved in 12 mL of NMP and stirred magnetically for 48 h at 38 °C to reach degree of functionalisation (Df) = 15%, mols of CH/mols of HA repeating units. A similar procedure was performed with 200 mg of Ge^-TBA^+ and 20 mg of CH-Br dissolved in 34.8 mL of NMP (Df = 6%, mols of CH/mols of Ge repeating units). The final products, HA-CH and Ge-CH, were purified by dialysis and recovered through freeze-drying, achieving a yield of approximately 90%. To form nanohydrogels (NHs), HA-CH and Ge-CH were dispersed in bi-distilled water at a concentration of 1.5 mg/mL and kept under magnetic stirring overnight at room temperature, according to a well-proven process described in previous works [12,25]. The resulting suspensions were then subjected to a standard sterilization cycle in an autoclave (121 °C, 20 min, at 1.10 bar) using a Juno Liarre autoclave (230 Vac, 50/60 Hz, 12 A, 2000 W). The formation of NHs was assessed using dynamic light scattering analysis. The size and ζ-potential were measured by using a Zetasizer Nano Z instrument (Malvern Instruments, UK) equipped with a solid state HeNe laser (λ = 633 nm) at a scattering angle of 173°.

2.4. Growth curve assay

To evaluate the bacterial duplication rate, 100 μL from an overnight bacterial culture (about 10^8 cells) was diluted 1:100 in a tube containing 10 mL of fresh BHI medium. For each strain, the bacteria were grown either in the presence and in the absence of HA-CH NHs and Ge-CH NHs, respectively. Additionally, the non-derivatized polymers (HA and Ge) were tested as controls. The tubes were incubated at 37 °C for 24 h with vigorous agitation at 180 rpm. Bacterial growth was monitored spectrophotometrically at a wavelength of 600 nm.

2.5. Biofilm formation

The effects of HA-CH and Ge-CH nanohydrogels (NHs) on biofilm formation by *S. epidermidis* were studied in vitro using a microtiter plate biofilm assay [10,32]. A sterile 96-well flat-bottom polystyrene plate was prepared, with the first row filled with 100 μL of BHI solution containing bacteria diluted at 1:100 from an overnight culture to establish baseline biofilm formation. In the second row, wells were filled with BHI medium containing bacteria at the same 1:100 dilution along with NHs at a concentration of 0.5 mg/mL. As a control, non-derivatized polymers were also tested at the equivalent concentration. From the second row onward, a series of 1:2 serial dilutions with BHI were performed, decreasing the NHs concentration to 0.007 mg/mL. The plates were then incubated under static conditions at 37 °C. After 24 h, the supernatant was aspirated, and the wells were washed twice with water to remove planktonic cells. Once dried, the residual biofilm was quantified by adding 100 μL of 0.1% (*w/v*) crystal violet solution to each well and incubating for 15 min at room temperature. The excess dye was removed by rinsing with water, and the wells were allowed to dry. The remaining crystal violet was solubilized using a solution of 20% (*v*/v)

acetone and 80% (v/v) ethanol. After incubating for 10 min at room temperature with constant agitation, the total biofilm biomass was spectrophotometrically quantified at a wavelength of 590 nm.

2.6. Biofilm timing assay

The NHs were evaluated at various stages of biofilm development: specifically, at 0 h, 2 h, 4 h, 6 h, and 24 h. At each phase of biofilm formation, the wells were categorized into treated and untreated groups. For the 0 h time point, the assay was conducted according to previously established methods. For the subsequent time points (2 h, 4 h, 6 h, and 24 h), biofilm formation was initiated by inoculating BHI medium with bacteria diluted at a ratio of 1:100. After the designated incubation periods, the supernatants were removed and replaced with BHI supplemented with NHs (0.5 mg/mL) in the treated wells, while the untreated wells received fresh medium and newly incubated at 37 °C overnight. The residual biofilm was quantified using 0.1% (w/v) crystal violet solution, following the previously described protocol.

2.7. Surface coating assay

The surface coating assay was performed as previously described [5], with some modifications. Four materials that are commonly used in hospital settings—titanium, glass, steel, and polystyrene—were selected for testing. Discs made from these materials were placed in the wells of a 24-well polystyrene microtiter plate. A volume of 5 μL of NHs suspensions (HA-CH, Ge-CH) at a concentration of 0.5 mg/mL was applied to the center of each disc and allowed to dry under sterile conditions at 37 °C for 1 h. Following this, 1 mL of *S. epidermidis* suspension (diluted 1:100 in BHI medium) was added to each well, to completely cover the surface of the coated discs. The plate was then incubated overnight at 37 °C. After 24 h, the wells were gently rinsed with water, and photographs were taken.

2.8. Surface protein extraction

To investigate structural changes in the surface of *S. epidermidis* following treatment, surface protein extraction was performed. Surface proteins were isolated using the Tabouret method [7,38], with minor modifications as described below. Non-derivatized polymers (HA and Ge) were used as controls. For the untreated sample, 10 mL of bacterial suspension (overnight culture 1:100 diluted in BHI) were placed in 50 mL tube. For the treated samples, to 10 mL of bacterial culture, obtained from an overnight culture 1:100 diluted in fresh BHI, a solution of each NH at final concentration of 0.125 mg/mL, was added. The flasks were incubated at 37 °C (60 rpm) until the cultures reached the exponential growth phase of $OD_{600} \approx 0.6$. The bacterial cultures were then centrifugated at 5000 rpm for 15 min at 4 °C. The supernatants were removed, and the obtained pellets were washed with 5 mL of PBS, followed by centrifugation under the same conditions. This washing step was repeated twice. Subsequently, each pellet was resuspended in 100 μL of PBS containing 1% SDS and incubated at 37 °C for 15 min. Lastly, the samples were centrifuged at 10000 rpm for 10 min at 4 °C, and the resulting supernatants were collected and stored at −20 °C. Protein profiles were then analyzed by polyacrylamide gel electrophoresis under denaturing conditions (SDS-PAGE).

2.9. Surface protein analysis

2.9.1. SDS-page

The previously prepared samples were used to perform SDS-PAGE (Sodium Dodecyl Sulphate - Polyacrylamide Gel Electrophoresis). Protein samples were mixed with Laemmli buffer containing 1 mM dithiothreitol (DTT) as a reducing agent and then denatured at 95 °C for 5 min. The samples were separated on a SDS-PAGE gel containing 10% of polyacrylamide with a 4% polyacrylamide stacker. Electrophoresis was conducted in Tris/glycine/SDS running buffer (pH 8.3) at 180 V for 40 min. Prestained molecular mass marker was included (mPAGE Color Protein Standard).

After electrophoresis run, the gel was incubated for 1 h in a fixing solution containing 40% ethanol (*v*/v) and 10% acetic acid (v/v), then washed twice with water for 10 min each. Protein bands were subsequently stained with Coomassie colloidal Brilliant Blue containing 10% (*w/v*) $(NH_4)_2SO_4$, 1% (v/v) H_3PO_4, and 0.25% (w/v) of the Coomassie G-250. The gels were stained for about 20 h in the previously described staining solution diluted with 20 (v/v) ethanol. Excess Coomassie stain was removed by washing the gels in distilled water [30]. The gel image was acquired using ChemiDoc imaging system.

2.9.2. Zymography

A zymography assay was conducted to examine the presence of hydrolytic enzymes in the extracted proteins. The primary difference between SDS-PAGE and zymography lies in the inclusion of a substrate, specifically *Micrococcus luteus* at a concentration of 0.2%, in the resolving phase of the gel. This allows for the detection of hydrolytic activity in the protein samples. Protein samples were mixed with Laemmli buffer without DTT and then denatured at 95 °C for 5 min. The electrophoretic run was performed simultaneously with the SDS-PAGE. After the run, the gel was washed with water and renatured in a solution of 1% Triton X-100 and 50 mM Tris-HCl (pH 8) at 37 °C with gentle agitation for 24 h. Following this incubation, the gels were stained with Colloidal Coomassie Brilliant Blue R-250. Hydrolytic activity was visualized as clear or transparent bands against a uniformly blue opaque gel, indicating regions where active proteins had degraded the substrate.

2.9.3. In situ digestion

The protein band from the untreated sample (NT of *S. epidermidis* O47), the protein band from the sample treated with hyaluronic acid (HA of *S. epidermidis* O47), and the corresponding area in the HA-CH NHs lane between 100 and 130 kDa were selected and excised from the SDS-PAGE and initially washed with acetonitrile (ACN), followed by washing with 0.1 M ammonium bicarbonate. The protein samples were then reduced by incubating them with 10 mM DTT for 45 min at 56 °C. Cysteines were alkylated by treating the samples with 5 mM iodoacetamide for 15 min at room temperature in the dark.

Next, the gel particles were washed again with ammonium bicarbonate and ACN. Tryptic digestion was performed using 10 μL of a solution containing 20 ng/mL of enzyme in 10 mM ammonium bicarbonate (pH 8.5) at 4 °C for 4 h. After this, the buffer solution was removed, and a new aliquot of the enzyme/buffer solution was added for an additional 18 h at 37 °C. The minimum reaction volume was used to ensure complete rehydration of the gel.

2.9.4. NanoLC mass spectrometry

When necessary, peptide mixtures were analyzed using LC-MS/MS with an LTQ Orbitrap XL Hybrid Ion Trap-Orbitrap mass spectrometry system. Analysis was conducted on a C18 capillary reverse-phase column (200 mm, 75 μm, 5 μm) at a flow rate of 250 nL/min. A step gradient was applied using eluent B (0.2% formic acid in 95% acetonitrile, LC-MS grade) and eluent A (0.2% formic acid in 2% acetonitrile), transitioning from 5% to 50% eluent B over 80 min and then to 80% over the next 5 min.

Mass spectrometry analyses were performed in data-dependent acquisition (DDA) mode over the m/z range of 400 to 1800, with a resolution set at 60,000. The automatic gain control (AGC) target was set to 1×10^6, followed by MS/MS acquisition of the five most abundant ions. For the MS/MS scans, the resolution was set to 15,000, the AGC target was set to 1×10^5, the precursor isolation width was 2 Da, and the maximum injection time was 500 ms. The normalized collision energy for collision-induced dissociation (CID) was set at 35%, with the AGC target maintained at 1×10^5.

The mass spectrometry proteomics data have been deposited to the

ProteomeXchange Consortium via the PRIDE partner repository with the dataset identifier PXD074516.

2.9.5. MASCOT analysis

The acquired MS/MS spectra were converted to Mascot Generic files (.mgf) format and subsequently queried against SwissProt (561,911 sequences; 202,173,710 residues) using a licensed version of Mascot software (version 2.4.0) available at www.matrixscience.com for protein identification. Standard parameters used in the searches included taxonomy *S. epidermidis,* trypsin as the enzyme, allowing for up to 3 missed cleavages, a 10 ppm MS tolerance, and a 0.6 Da MS/MS tolerance, with peptide charges ranging from +2 to +4. Carbamidomethylation of cysteines was set as the sole fixed chemical modification, while possible oxidation of methionines and formation of pyroglutamic acid from glutamine residues at the N-terminal position of peptides were considered as variable modifications.

2.10. Eukaryotic cell lines and culture conditions

The mouse leukemic monocyte-macrophage (RAW 264.7 cells) and human osteoblast (MG-63 cells) were used in this study. Cells were maintained in Dulbecco's Modified Eagle Medium (DMEM, high glucose, 4.5 g/L; Sigma-Aldrich S.r.l, Milan, Italy) supplemented with 10% (*v*/v) heat-inactivated fetal bovine serum (FBS), 1% (v/v) L-glutamine (200 mM), and 1% (v/v) penicillin–streptomycin (10,000 U/mL penicillin; 10 mg/mL streptomycin). Cultures were incubated at 37 °C in atmosphere containing 5% CO_2. Confluent monolayers were used 24 h after seeding.

2.11. Cell viability assay

The cytotoxicity of NHs was evaluated in mouse leukemic monocyte-macrophage (RAW 264.7 cells) and human osteoblast (MG-63 cells) using the MTT Cell Proliferation Kit (Roche Applied Science, Penzberg, Germany). Following cells seeding, both cell lines were incubated at 37 °C in a 5% CO_2 atmosphere for 4, 12, and 24 h, either in the presence or absence of treatment. After incubation, 100 μL of basal medium containing MTT (0.5 mg/mL) was added to each well and the plates were incubated for an additional 4 h. Formation of purple formazan crystals was verified microscopically (40× magnification). The medium was then carefully removed, and 100 μL of DMSO was added to solubilize the formazan. After 15 min of incubation at 37 °C, absorbance at 570 nm was measured using a Tecan Infinite 200 Pro microplate reader.

Cell viability was calculated as the percentage of metabolically active cells in the presence of the different NHs (HA-CH and Ge-CH) compared to untreated controls. Control cells were cultured without NHs and supplemented with identical volumes of DMSO.

3. Results

3.1. Preparation and characterization of HA-CH and Ge-CH NHs

The grafting of HA and Ge with cholesterol moieties to obtain amphiphilic polymers HA-CH and Ge-CH able to self-assemble in soft nanosystems was extensively described in previous papers [12,22,25].

HA-CH and Ge-CH with a stoichiometric degree of derivatization (DD %) of respectively 15% and 6% were selected, following an optimization process, because they exhibited an optimal balance between hydrophilic and lipophilic moieties, which enabled their organization into nanosystems. A characterization of the derivatives was carried out by NMR spectroscopy, as reported in previous studies [24].

To facilitate the self-assembly of HA-CH and Ge-CH, the modified polysaccharide suspensions underwent a standard autoclave sterilization cycle (20 min at 121 °C and 1.10 bar). This process promotes a three-dimensional rearrangement of the polymers [25]. The temperature and pressure conditions enhance the interaction between the hydrophobic regions of the chains, resulting in the formation of inner lipophilic domains. Meanwhile, the polysaccharide chains are structured on the outside, interacting with water and minimizing free interfacial energy. A drawing illustrating the formation and structure of nanohydrogels (NHs) is shown in Fig. 1. This nanohydrogels were extensively characterized for drug delivery application and proven to be in the range of nanometers; moreover, cryo-TEM images have revealed a homogeneous surface and round shape of the nanosystems [24].

As a result, sterile aqueous formulations of HA-CH NHs and Ge-CH NHs can be easily obtained, making them ready for bacterial testing. The HA-CH and Ge-CH NHs were characterized using dynamic light scattering. The HA-CH NHs exhibited a mean size of 288 ± 5 nm, with a polydispersity index (PDI) of 0.23 ± 0.02, and a ζ-potential of −40.7 ± 2.18 mV. In contrast, the Ge-CH NHs measured 178 ± 1 nm in size, with a PDI of 0.25 ± 0.02, and a ζ-potential of −19.7 ± 2.84 mV. As previously reported, both types of nanogels remain stable at both 37 °C and 4 °C for up to one month [25].

3.2. Influence of NHs on duplication rate of S. epidermidis

Before analyzing the impact of NHs on biofilm formation by *S. epidermidis*, we first assessed their influence on bacterial growth curves to rule out any potential effect on the rate of bacterial duplication. The growth curves were established both in the presence and absence of NHs and native polymers (HA and Ge) as controls, at a concentration of 0.5 mg/mL. As shown in Fig. 2, the curves in graphs a and b are superimposable. This indicates that neither the polymers nor the corresponding NHs affected the growth of the two tested bacterial strains, effectively ruling out any impact on the rate of bacterial cell duplication.

3.3. Effect of HA-CH and Ge-CH NHs on S. epidermidis biofilm formation

The anti-biofilm activity of nanoparticles (NHs) and native polymers was evaluated using a microtiter plate assay (MTP) at various concentrations, starting from 0.5 mg/mL. Biofilm formation was quantified using a crystal violet assay and spectrophotometrically measured at 590 nm. As shown in Fig. 3a, regarding biofilm formation by *S. epidermidis* ATCC O47, NHs demonstrated a greater efficacy than the native polymers at the same concentration, highlighting the importance of the nanoparticle form of the polymers. At 0.5 mg/mL, HA-CH and Ge-CH NHs inhibited significantly biofilm formation by approximately 90% in comparison to the non-treated samples. Furthermore, a dose-dependent effect was observed: higher concentrations corresponded to a proportional increase in anti-biofilm efficacy. It is important to note that no benefits were observed from using non-derivatized HA. In contrast, while non-derivatized Ge exhibited anti-biofilm efficacy, it was lower than that of the corresponding NHs but still significantly relevant. Regarding the results obtained with *S. epidermidis* ATCC RP62A strain, as shown in Fig. 3b, the NHs demonstrated significant anti-biofilm activity, preventing biofilm formation by approximately 60% and 70% compared to the control sample, respectively for HA-CH and Ge-CH NHs. Native Ge also produced interesting results, and together with the nanogels, they

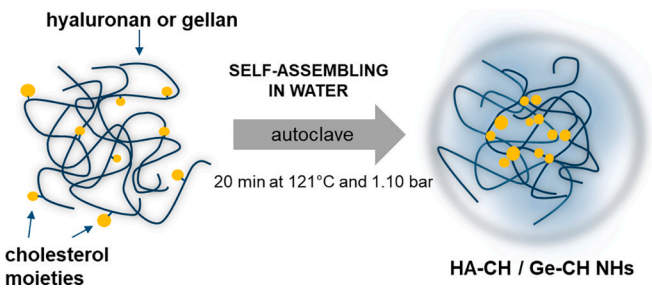

Fig. 1. Self-assembling process of HA-CH and Ge-CH to obtain NHs.

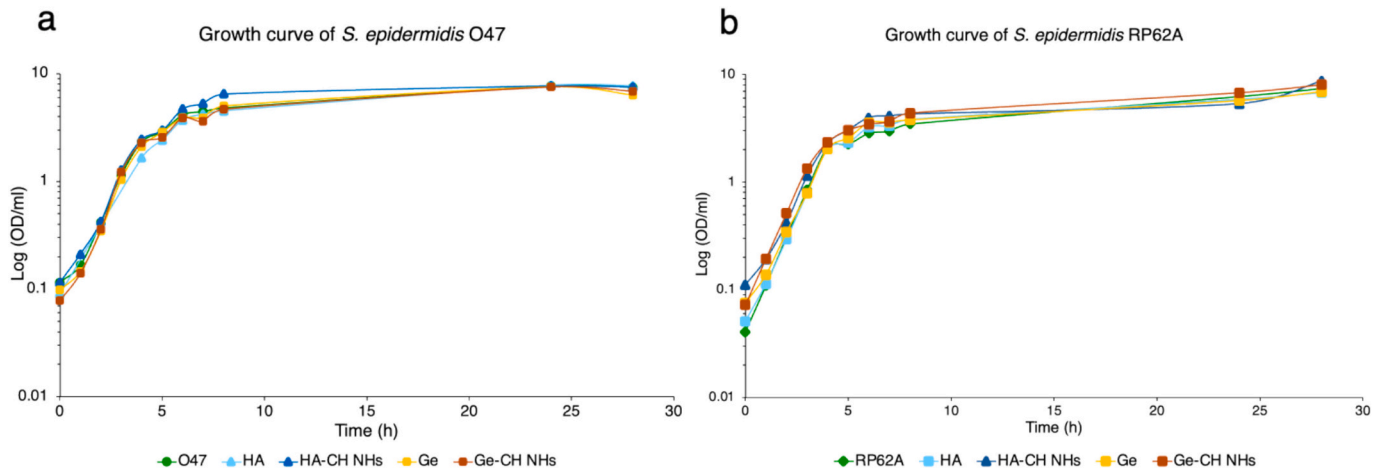

Fig. 2. Growth curves of *S. epidermidis* ATCC strains O47 (a) and RP62A (b). The bacterial strains were grown at 37 °C under constant agitation (180 rpm) in BHI medium in the absence and in the presence of HA, HA-CH NHs, Ge and Ge-CH NHs (0.5 mg/mL), respectively. The bacterial culture was spectrophotometrically monitored at 600 nm over a period of 28 h.

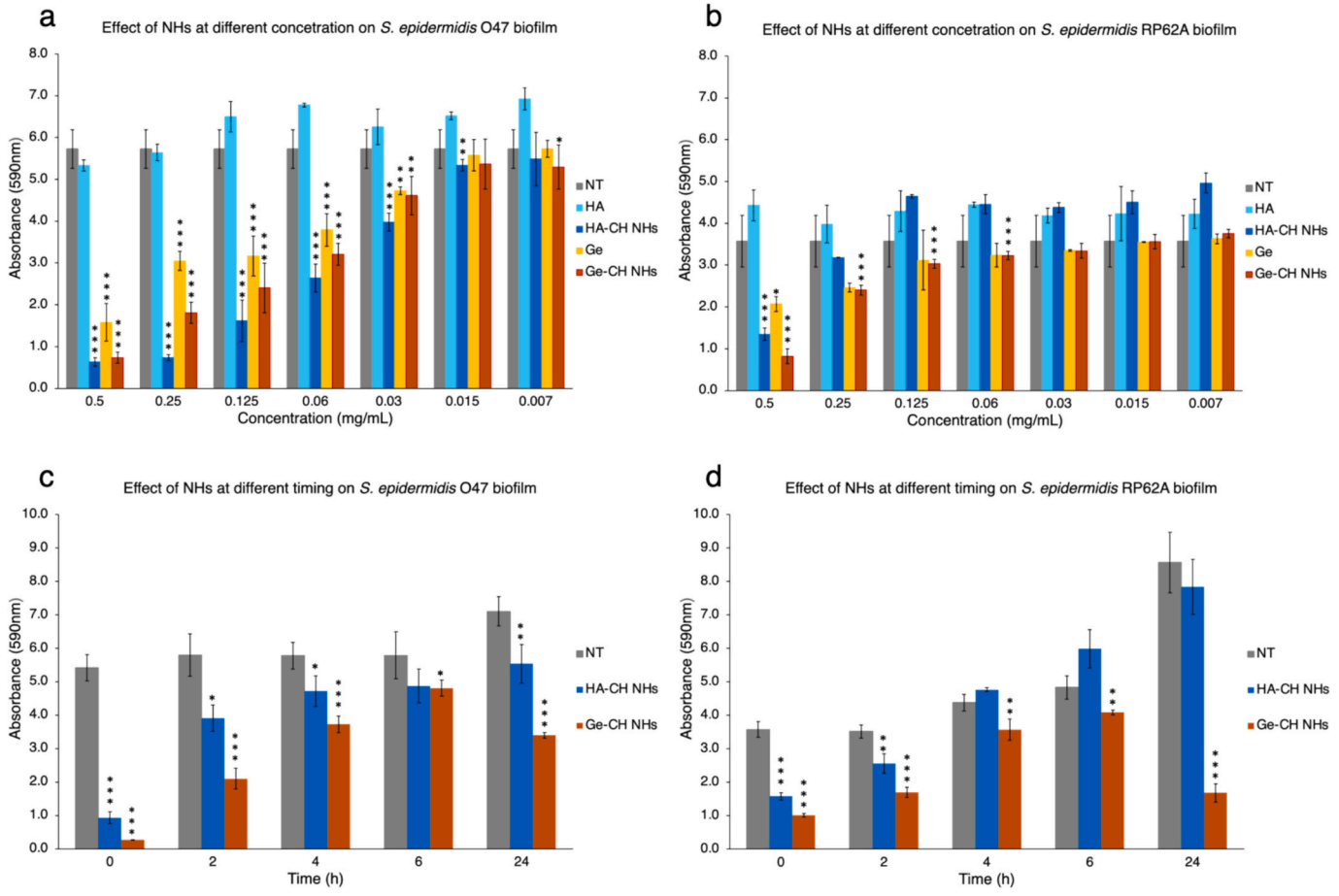

Fig. 3. **a-b** Effect of HA, HA-CH NHs, Ge, and Ge-CH NHs at different concentrations against *S. epidermidis* ATCC O47 and RP62A biofilm formation. The activity of NHs and polymers was tested at time 0 h of biofilm formation. Biofilm formation was evaluated after 24 h of incubation at 37 °C in polystyrene plates. **c-d** Effect of the HA-CH and Ge-CH NHs (0.5 mg/mL) added at different times of biofilm formation of *S. epidermidis* ATCC O47 and RP62A. Biofilm formation was evaluated after 24 h of incubation at 37 °C in polystyrene plates. Data are reported as OD at 590 nm after crystal violet staining. NT: not-treated sample. Each data point represents the mean ± SD of 4 independent experiments, each performed in 6-replicates. Statistical analysis was performed using the Student's ***t***-test. Differences were considered significant at $p < 0.05$ (*), $p < 0.01$ (**), **and** $p < 0.001$ (***), compared with the control.

both exhibited the same dose-dependent relationship seen with the ATCC O47 strain. HA did not show any anti-biofilm activity, while HA-CH NHs were effective only at the higher tested concentrations.

A timing assay was conducted to assess the impact of NHs during various stages of biofilm formation (Fig. 3c-d). In this experiment, the nanogels were introduced into the bacterial cultures at a concentration

of 0.5 mg/mL at different time points. The final time point, 24 h, represents a well-structured and mature biofilm, at which point the disruption capability of the NHs was evaluated. As shown in Fig. 3c-d, the effect of NHs on both bacterial strains was time-dependent, demonstrating greater effectiveness during the initial phases of biofilm adhesion (0 h). In this first stage, biofilm impairment ranged from 60% to 90%. At the 24-h mark, when the disruptive activity can be assessed, a significant reduction in the mature biofilm for both strains was observed. Best results were obtained with Ge-CH NHs on ATCC RP62A strain, which resulted in approximately an 80% decrease.

3.4. Anti-adhesion activity of NHs against S. epidermidis biofilm

A surface coating assay was conducted to further investigate the anti-adhesive properties of NHs, which had previously shown promising results in the timing assay. In this experiment, we analyzed the ability of NHs to inhibit bacterial adhesion on various surfaces commonly used in clinical settings, including titanium, stainless steel, glass, and polystyrene (PS). We placed 5 μL of each substance, at a concentration of 0.5 mg/mL, on the discs to be tested. The control experiment (NT) involved depositing sterile water on the discs. After the drop of substance had evaporated, the discs were immersed in a bacterial culture and incubated overnight at 37 °C under static conditions. The results are illustrated in Fig. 4. No differences in biofilm formation were observed on the control discs (NT) or those treated with hyaluronic acid (HA). In contrast, the discs treated with Ge, Ge-CH NHs, and HA-CH NHs exhibited a complete lack of bacterial adhesion where the nanogel suspension was deposited, across all materials tested.

3.5. Analysis of bacterial surface protein profile

To explain the anti-adhesive properties of non-hydrophobic nanoparticles (NHs) at the molecular level, we analyzed the surface protein patterns of *S. epidermidis* strains, which are known to play a crucial role in the adhesion process on both biotic and abiotic surfaces [16]. The protein samples, derived from bacterial cultures grown with and without polymers and corresponding NHs, were qualitatively analyzed using SDS-PAGE. We used a concentration of NHs at 0.125 mg/mL, as higher concentrations of Ge and Ge-CH NHs made it difficult to separate proteins from cellular debris during centrifugation. Fig. 5 shows the SDS-PAGE electrophoretic profiles of the protein patterns obtained from surface protein extracts by *S. epidermidis* strains following Coomassie blue staining (left panel) and after the autolytic pattern analysis (right panel).

As shown in Fig. 5 **a** and **b**, the protein profiles of treated and untreated samples were similar for both bacterial strains, except for samples extracted from the cells grown in the presence of HA-CH NHs, where a drastic reduction in the numbers of protein bands was observed. In particular, the disappearance of a protein band with apparent molecular between 100 and 130 KDa was observed.

The autolytic profiles of treated and untreated surface proteins extracted from *S. epidermidis* were in accordance with the results observed in SDS-PAGE analysis (Fig. 5 **c** and **d**), confirming the disappearance of an autolytic band in the sample extracted from the cells grown in the presence of HA-CH NHs with apparent molecular between 100 and 130 KDa.

This protein band from the untreated sample (NT of *S. epidermidis* O47), the protein band from the sample treated with hyaluronic acid (HA of *S. epidermidis* O47), and the corresponding area in the HA-CH NHs lane, were excised from the SDS-PAGE gel and selected for further analyses. These samples were then subjected to in-situ trypsin hydrolysis and subsequently identified by LC-MS/MS with an LTQ Orbitrap XL Hybrid Ion Trap-Orbitrap mass spectrometry, which provides high-accuracy peptide mass measurements and enables the selective identification of peptides and proteins. This analysis revealed the presence of the protein adhesin/autolysin AtlE (with mascot scores of 1475 and 1910, respectively) only in the untreated sample and in sample treated with HA. AtlE is documented in the literature as playing a critical role in the adhesion phase of *S. epidermidis* biofilm formation [17,34]. Although the results are preliminary, the disappearance of this protein can suggest that NHs may influence the initial adhesion phase of the bacteria to the substrate, likely by targeting the AtlE adhesin/autolysin.

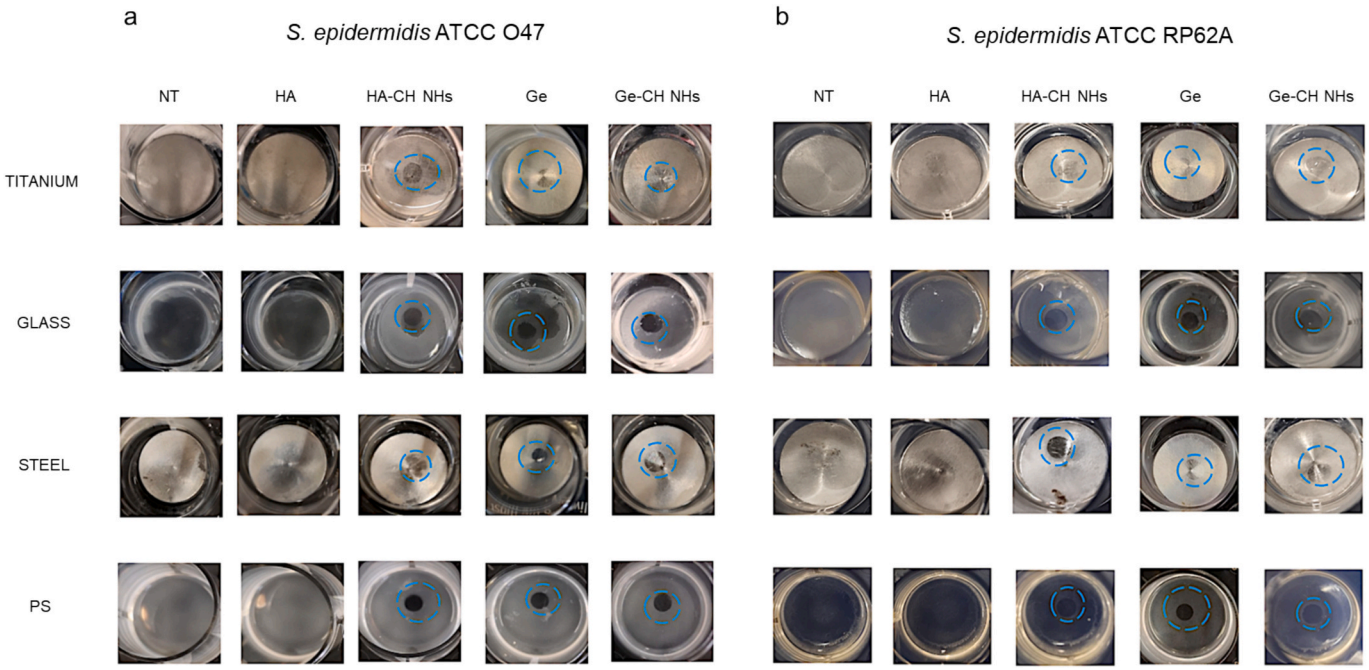

Fig. 4. Surface coating assay of *S. epidermidis*. The center of each disc was coated with liquid dispersions of each substance (HA, HA-CH NHs, Ge, Ge-CH NHs), and after solvent evaporation, the wells were then filled with bacterial culture in BHI and incubated 24 h at 37 °C in static conditions. Stained biofilms were rinsed with water and dried, and the wells were photographed. Blue circles indicate the inhibition halo of bacterial adhesion. NT: control sample. **a:** *S. epidermidis* ATCC O47. **b:** *S. epidermidis* ATCC RP62A. (For interpretation of the references to color in this figure legend, the reader is referred to the web version of this article.)

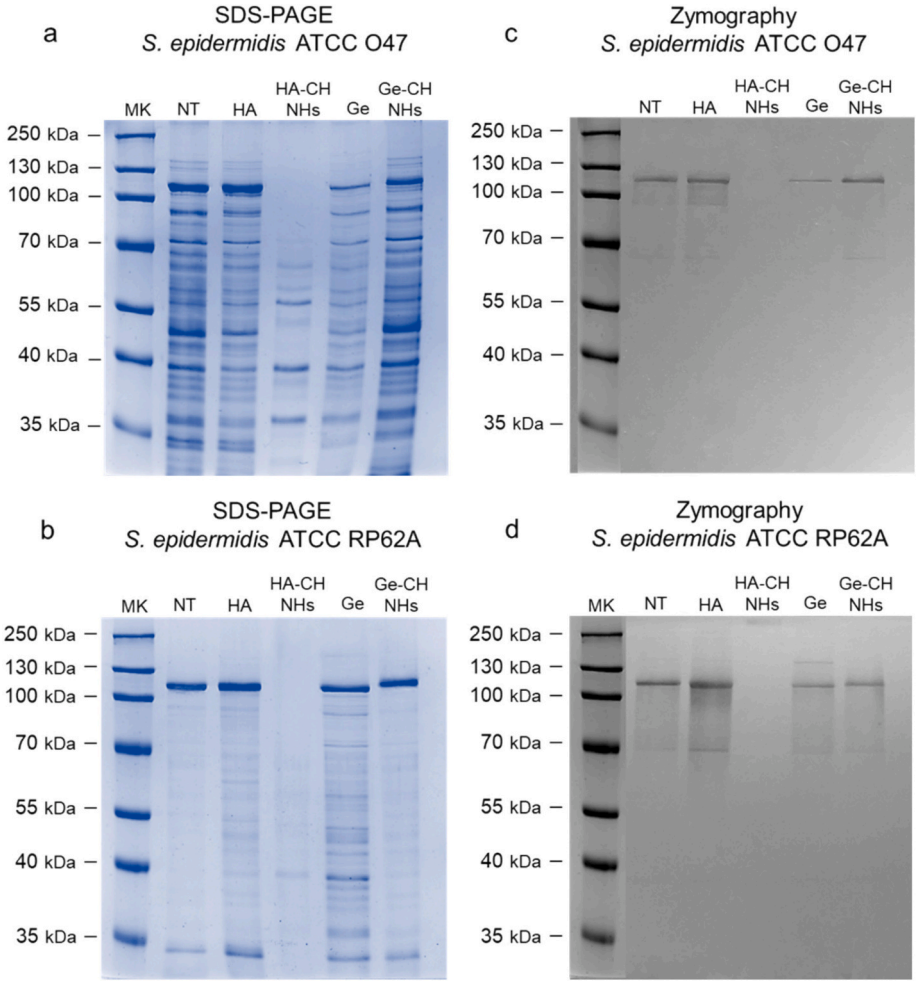

Fig. 5. Analysis of surface protein patterns of *S. epidermidis* ATCC O47 and RP62A. a and b: SDS-PAGE. c and d: Zymography. MK: Protein molecular weight marker. NT: proteins extracted from untreated cultures. HA, HA-CH NHs, Ge and Ge-CH NHs: proteins extracted from treated cultures (0.125 mg/mL).

3.6. *Effect of HA-CH and Ge-CH NHs on eukaryotic cell viability*

The biocompatibility of NHs was investigated by performing a cytotoxicity assay on mouse leukemic monocyte-macrophage (RAW 264.7 cells) and human osteoblast (MG-63 cells). These two cell lines were selected to evaluate the potential effects of NHs on different cellular models. Cells were incubated with HA-CH NHs and Ge-CH NHs at the highest tested concentration (0.5 mg/mL) for 4, 12, and 24 h, and cell viability was subsequently assessed using the MTT assay.

As shown in Fig. 6, no cytotoxic effects were observed in either cell

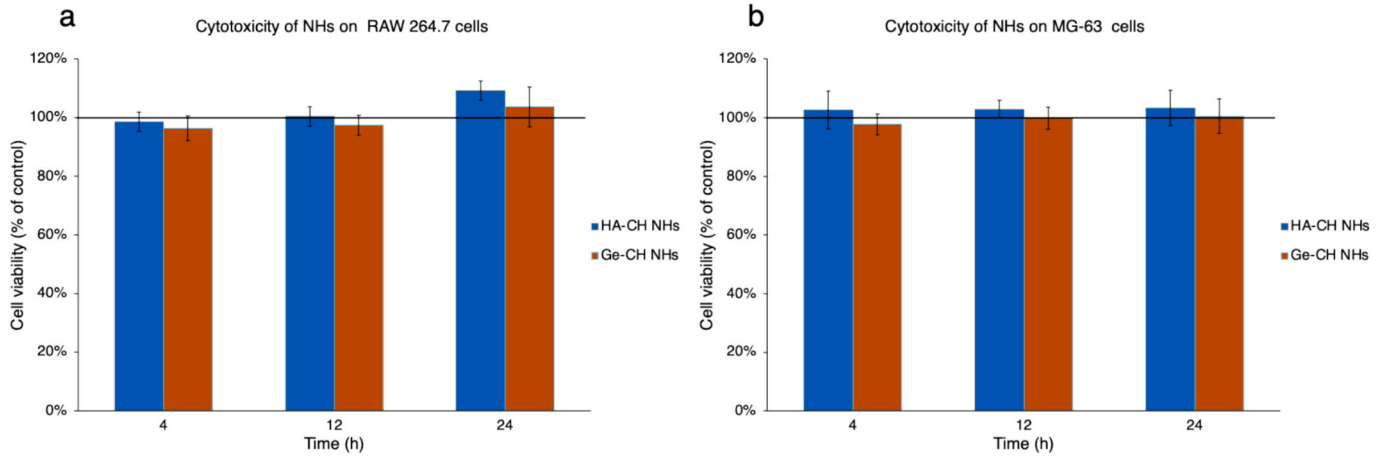

Fig. 6. Effect of HA-CH and Ge-CH NHs on RAW 264.7 (a) and MG-63 (b) cell lines. Cells were incubated with NHs at 0.5 mg/mL for 4, 12, and 24 h, and cell viability was measured using the MTT assay as described in the Materials and Methods section. The percentages of viable cells remained high across all time points for both cell lines, with no significant reduction observed relative to untreated controls. Statistical analysis was performed using the Student's *t*-test.

line under the tested conditions. The percentage of viable cells remained consistently high, with values approaching 100% viability at 4, 12, and 24 h, compared with untreated controls. These results indicate that both NHs are highly biocompatible and do not compromise the viability of the tested cell types, supporting their potential use in biomedical applications.

4. Discussion

The increasing antibiotic resistance of bacteria poses a significant challenge in treating infections, particularly in hospitals where multidrug-resistant strains commonly cause nosocomial infections [11]. This urgency highlights the need for alternative therapies that can effectively combat infections that do not respond to traditional pharmacological methods. One promising approach is to target bacterial virulence factors, which are the mechanisms pathogens use to establish and persist within the host. These factors help bacteria evade immune responses, acquire nutrients, strengthen colonization, and damage host cells [9,14]. Among various virulence factors, bacterial biofilms play a crucial role. They allow microorganisms to avoid the immune system response and significantly enhance their resistance to drugs; bacteria within a biofilm can be up to 1000 times more resistant to antimicrobials than their free-floating (planktonic) counterparts [28]. While most research focuses on discovering new antibiotics or improving the effectiveness of existing ones, there is currently no therapy specifically designed to target bacterial biofilms or other virulence factors.

One of the leading causes of nosocomial infections associated with indwelling medical devices is *S. epidermidis*, a commensal bacterium commonly found in the human skin microbiome. This bacterium is often resistant to multiple conventional antimicrobial therapies and is typically associated with biofilm formation [47]. For this study, we selected two well-characterized reference strains, ATCC 047 and RP62A, which are known for their ability to produce significant amounts of biofilm [35,41].

HA-CH and Ge-CH NHs have been extensively studied as drug delivery systems and offer various advantages from several perspectives [3,12,22,23,25–27,42,43,48]. They are both biocompatible and biodegradable, allowing them to effectively encapsulate a wide range of substances. Additionally, the raw materials required for their synthesis are readily available. Furthermore, cytotoxicity and stability studies have already been conducted, yielding promising results that underscore the potential of these systems [13,24].

We investigated the anti-biofilm activity of unloaded polysaccharide-based nanohydrogels (NHs), a topic that has not been previously explored. The results indicated that the HA-CH and Ge-CH nanohydrogels effectively reduced biofilm production without impacting bacterial growth or vitality. Their effectiveness was found to be both time- and concentration-dependent for both tested strains of *S. epidermidis*. Timing assays revealed that the nanogels primarily act during the initial adhesion stage of biofilm formation, though they also show potential for disaggregating mature biofilms. Our tests highlighted the significance of the nanoparticle formulation of these polymers, particularly in the case of HA, as similar outcomes were not observed with non-derivatized and non-nanoparticle polymers. Perhaps, the NHs could have an amphiphilic nature that facilitates a more effective association with bacterial surface and biofilm matrix compared to the purely hydrophilic polymers. Also, the increase in the effective dimensions and local density of the polymer chains in the NHs form leads this supramolecular organization to specific steric or chemical interactions that are not possible for individual, non-assembled polymer chains in solution. Furthermore, we examined the anti-adhesive action of these nanogels on several materials commonly used in hospitals. For instance, stainless steel is frequently used for surgical instruments and implants, such as artificial heart valves and orthopedic devices, while titanium serves similar purposes [18]. Polystyrene is not directly used in the manufacturing of implantable medical devices, but it is commonly found in packaging for laboratory instruments, medical device casings, test tubes, and surgical tools due to its versatility. Additionally, glass is utilized in medical equipment and laboratory tools because of its transparency, chemical resistance, and easy of sterilization [4,46]. While these materials provide a non-porous surface that helps prevent the spread of infections, they can still serve as surfaces for biofilm adhesion. Therefore, an innovative strategy could involve coating medical devices with substances that inhibit adhesion and biofilm formation [36,44]. Our results indicated that Ge and both types of nanogels demonstrated anti-adhesive properties on all tested materials; indeed, biofilms were uniformly present on the different discs except at the locations where the substances were applied. This could represent a significant breakthrough in the development of implantable medical systems, which are often sites for biofilm formation and persistent infections sustained by *S. epidermidis*.

At a molecular level, surface protein analysis of *S. epidermidis* strains revealed the disappearance of the adhesin/autolysin AtlE, only following the treatment with HA-CH NHs. This protein plays a crucial role in the adhesion phase of *S. epidermidis* biofilm formation. AtlE exhibits bifunctional activity: it catalyzes the cleavage of peptidoglycan to facilitate cell wall reorganization during adhesion and acts as an adhesin, promoting attachment to surfaces and stabilizing the initial interactions between the bacterium and the surface [17,34].

This finding suggests a potential target for HA-CH nanohydrogels (NHs), which may operate by depleting or modifying the structure of AtlE, thereby eliminating its hydrolytic activity. It also raises the possibility of an alternative target for Ge-CH NHs, which, despite affecting biofilm formation, do not weaken AtlE. Parallel studies conducted in our laboratory demonstrated that Ge-CH NHs exhibits a broad-spectrum antibiofilm efficacy not only limited to *Staphylococcus* genus, unlike the more selective HA-CH NHs (unpublished data). We can speculate that the activity of Ge-CH NHs is likely driven by non-specific interactions rather than target-specific molecular binding. Our hypothesis is that Ge-CH NHs interact with the architecture of biofilm, specifically on matrix structure. Moreover, the assessment of the cellular biocompatibility of the NHs systems was broadened beyond previously reported studies performed on the parental human melanoma cell line M14, its multidrug-resistant variant M14 ADR2, and the human ovarian cancer cell line HeLa [13,24]. In the present work, we extended the investigation to mouse leukemic monocyte-macrophage (RAW 264.7 cells) [33] and human osteoblast (MG-63 cells) [37], further confirming the high biocompatibility of these nanogels.

5. Conclusions

In conclusion, the promising results indicate that the use of HA-CH and Ge-CH nanohydrogels could serve as an alternative strategy for preventing or treating biofilm infections associated with *S. epidermidis*. One of the future goals will be to formulate these NHs by incapsulating conventional antibiotics. This approach would combine two different strategies: the breakdown of biofilms and the targeted delivery of drugs to the site of infection, reducing toxicity and enhancing the potential for synergistic activity between NHs and antibiotics.

CRediT authorship contribution statement

Anna Pietrella: Writing – original draft, Methodology, Investigation, Data curation. **Irene Paris:** Writing – original draft, Validation, Methodology, Investigation, Data curation. **Claudia Migliorini:** Validation, Investigation, Data curation. **Marco Morelli:** Investigation, Data curation. **Andrea Carpentieri:** Validation, Data curation. **Pietro Matricardi:** Validation, Supervision, Project administration, Methodology, Funding acquisition. **Chiara Di Meo:** Writing – review & editing, Validation, Supervision, Project administration, Methodology, Funding acquisition, Conceptualization. **Rosanna Papa:** Writing – review & editing, Validation, Supervision, Project administration, Methodology,

Funding acquisition, Conceptualization.

Funding

This research was funded by the Sapienza University of Rome "Finanziamenti di Ateneo per la Ricerca Scientifica" - RM1221813859CA94 and RM123188E3C29FE2.

Declaration of competing interest

The authors declare no competing interests.

Data availability

Data will be made available on request.

References

[1] A.A. Ali, R.D. Al Bostami, A. Al-Othman, Nanogel-based composites for bacterial antibiofilm activity: advances, challenges, and prospects, RSC Adv. 14 (15) (2024) 10546–10559, https://doi.org/10.1039/D4RA00410H.
[2] D. Allen-Taylor, G. Boro, P.M. Cabato, C. Mai, K. Nguyen, G. Rijal, *Staphylococcus epidermidis* biofilm in inflammatory breast cancer and its treatment strategies, Biofilm 8 (2024) 100220, https://doi.org/10.1016/j.bioflm.2024.100220.
[3] I. Andreana, N. Zoratto, C. Di Meo, P. Matricardi, B. Stella, S. Arpicco, An overview of hyaluronic-acid nanoparticles for cancer cell targeted drug delivery, Expert Opin. Drug Deliv. 22 (9) (2025) 1257–1274, https://doi.org/10.1080/17425247.2025.2515266.
[4] C.R. Arciola, D. Campoccia, P. Speziale, L. Montanaro, J.W. Costerton, Biofilm formation in Staphylococcus implant infections. A review of molecular mechanisms and implications for biofilm-resistant materials, Biomaterials 33 (26) (2012) 5967–5982, https://doi.org/10.1016/j.biomaterials.2012.05.031.
[5] M. Artini, P. Cicatiello, A. Ricciardelli, R. Papa, L. Selan, P. Dardano, E. Parrilli, Hydrophobin coating prevents *Staphylococcus epidermidis* biofilm formation on different surfaces, Biofouling 33 (7) (2017) 601–611, https://doi.org/10.1080/08927014.2017.1338690.
[6] M. Artini, C. Romanò, L. Manzoli, G.L. Scoarughi, R. Papa, E. Meani, L. Selan, Staphylococcal IgM enzyme-linked immunosorbent assay for diagnosis of Periprosthetic joint infections, J. Clin. Microbiol. 49 (1) (2011) 423–425, https://doi.org/10.1128/JCM.01836-10.
[7] M. Artini, R. Papa, G.L. Scoarughi, E. Galano, G. Barbato, P. Pucci, L. Selan, Comparison of the action of different proteases on virulence properties related to the staphylococcal surface, J. Appl. Microbiol. 114 (1) (2013) 266–277, https://doi.org/10.1111/jam.12038.
[8] X. Ba, C.L. Raisen, O. Restif, L.M. Cavaco, C. Vingsbo Lundberg, J.Y.H. Lee, J. Larsen, Cryptic susceptibility to penicillin/β-lactamase inhibitor combinations in emerging multidrug-resistant, hospital-adapted *Staphylococcus epidermidis* lineages, Nat. Commun. 14 (1) (2023) 6479, https://doi.org/10.1038/s41467-023-42245-y.
[9] M.B. Calvert, V.R. Jumde, A. Titz, Pathoblockers or antivirulence drugs as a new option for the treatment of bacterial infections, Beilstein J. Org. Chem. 14 (2018) 2607–2617, https://doi.org/10.3762/bjoc.14.239.
[10] A. Casillo, R. Papa, A. Ricciardelli, F. Sannino, M. Ziaco, M. Tilotta, E. Parrilli, Anti-biofilm activity of a long-chain fatty aldehyde from Antarctic Pseudoalteromonas haloplanktis TAC125 against *Staphylococcus epidermidis* biofilm, Front. Cell. Infect. Microbiol. 7 (2017), https://doi.org/10.3389/fcimb.2017.00046.
[11] A.L. Costa, G.P. Privitera, G. Tulli, G. Toccafondi, Infection prevention and control (A c. Di), in: L. Donaldson, W. Ricciardi, S. Sheridan, R. Tartaglia (Eds.), Textbook of Patient Safety and Clinical Risk Management, Springer International Publishing, Cham, 2021, pp. 99–116, https://doi.org/10.1007/978-3-030-59403-9_9.
[12] G. D'Arrigo, C.D. Meo, E. Gaucci, S. Chichiarelli, T. Coviello, D. Capitani, P. Matricardi, Self-assembled gellan-based nanohydrogels as a tool for prednisolone delivery, Soft Matter 8 (45) (2012) 11557–11564, https://doi.org/10.1039/C2SM26178B.
[13] G. D'Arrigo, G. Navarro, C.D. Meo, P. Matricardi, V. Torchilin, Gellan gum nanohydrogel containing anti-inflammatory and anti-cancer drugs: a multi-drug delivery system for a combination therapy in cancer treatment, Eur. J. Pharm. Biopharm. 87 (1) (2014) 208–216, https://doi.org/10.1016/j.ejpb.2013.11.001.
[14] R. Dehbanipour, Z. Ghalavand, Anti-virulence therapeutic strategies against bacterial infections: recent advances, Germs 12 (2) (2022) 262–275, https://doi.org/10.18683/germs.2022.1328.
[15] V. Dengler Haunreiter, M. Boumasmoud, N. Häffner, D. Wipfli, N. Leimer, C. Rachmühl, A.S. Zinkernagel, In-host evolution of *Staphylococcus epidermidis* in a pacemaker-associated endocarditis resulting in increased antibiotic tolerance, Nat. Commun. 10 (1) (2019) 1149, https://doi.org/10.1038/s41467-019-09053-9.
[16] T.J. Foster, Surface proteins of *Staphylococcus epidermidis*, Front. Microbiol. 11 (2020) 1829, https://doi.org/10.3389/fmicb.2020.01829.
[17] C. Heilmann, M. Hussain, G. Peters, F. Götz, Evidence for autolysin-mediated primary attachment of *Staphylococcus epidermidis* to a polystyrene surface, Mol. Microbiol. 24 (5) (1997) 1013–1024, https://doi.org/10.1046/j.1365-2958.1997.4101774.x.
[18] H. Koseki, T. Shida, I. Yoda, H. Horiuchi, H. Sakoda, M. Osaki, Adherence ability of *Staphylococcus epidermidis* on prosthetic biomaterials: an in vitro study, Int. J. Nanomedicine (2013) 3955, https://doi.org/10.2147/IJN.S51994.
[19] D. Lebeaux, J.-M. Ghigo, C. Beloin, Biofilm-related infections: bridging the gap between clinical management and fundamental aspects of recalcitrance toward antibiotics, Microbiol. Mol. Biol. Rev. 78 (3) (2014) 510–543, https://doi.org/10.1128/MMBR.00013-14.
[20] P. Li, J. Pan, Y. Dong, Y. Sun, W. Yalong, K. Liao, H. Hu, Microenvironment responsive charge-switchable nanoparticles act on biofilm eradication and virulence inhibition for chronic lung infection treatment, J. Control. Release 365 (2023), https://doi.org/10.1016/j.jconrel.2023.11.032.
[21] Z. Liu, K. Guo, L. Yan, K. Zhang, Y. Wang, X. Ding, F.-J. Xu, Janus nanoparticles targeting extracellular polymeric substance achieve flexible elimination of drug-resistant biofilms, Nat. Commun. 14 (1) (2023) 5132, https://doi.org/10.1038/s41467-023-40830-9.
[22] E. Montanari, G. D'Arrigo, C. Di Meo, A. Virga, T. Coviello, C. Passariello, P. Matricardi, Chasing bacteria within the cells using levofloxacin-loaded hyaluronic acid nanohydrogels, Eur. J. Pharm. Biopharm. 87 (3) (2014) 518–523, https://doi.org/10.1016/j.ejpb.2014.03.003.
[23] E. Montanari, N. Zoratto, L. Mosca, L. Cervoni, E. Lallana, R. Angelini, P. Matricardi, Halting hyaluronidase activity with hyaluronan-based nanohydrogels: development of versatile injectable formulations, Carbohydr. Polym. 221 (2019) 209–220, https://doi.org/10.1016/j.carbpol.2019.06.004.
[24] E. Montanari, S. Capece, C. Di Meo, M. Meringolo, T. Coviello, E. Agostinelli, P. Matricardi, Hyaluronic acid Nanohydrogels as a useful tool for BSAO immobilization in the treatment of melanoma Cancer cells: hyaluronic acid Nanohydrogels as a useful tool …, Macromol. Biosci. 13 (9) (2013) 1185–1194, https://doi.org/10.1002/mabi.201300114.
[25] E. Montanari, M.C. De Rugeriis, C. Di Meo, R. Censi, T. Coviello, F. Alhaique, P. Matricardi, One-step formation and sterilization of gellan and hyaluronan nanohydrogels using autoclave, J. Mater. Sci. Mater. Med. 26 (1) (2015) 5362, https://doi.org/10.1007/s10856-014-5362-6.
[26] E. Montanari, A. Oates, C. Di Meo, J. Meade, R. Cerrone, A. Francioso, P. Matricardi, Hyaluronan-based nanohydrogels for targeting intracellular *S. aureus* in Human Keratinocytes, Adv. Healthc. Mater. 7 (12) (2018) e1701483, https://doi.org/10.1002/adhm.201701483.
[27] U.M. Musazzi, C. Cencetti, S. Franzé, N. Zoratto, C. Di Meo, P. Procacci, F. Cilurzo, Gellan Nanohydrogels: novel Nanodelivery Systems for Cutaneous Administration of Piroxicam, Mol. Pharm. 15 (3) (2018) 1028–1036, https://doi.org/10.1021/acs.molpharmaceut.7b00926.
[28] I. Olsen, Biofilm-specific antibiotic tolerance and resistance, Eur. J. Clin. Microbiol. Infect. Dis. 34 (5) (2015) 877–886, https://doi.org/10.1007/s10096-015-2323-z.
[29] M. Otto, *Staphylococcus epidermidis*—the "accidental" pathogen, Nat. Rev. Microbiol. 7 (2009) 555–567, https://doi.org/10.1038/nrmicro2182.
[30] R. Papa, S. Glagla, A. Danchin, T. Schweder, G. Marino, A. Duilio, Proteomic identification of a two-component regulatory system in *Pseudoalteromonas haloplanktis* TAC125, Extremophiles 10 (6) (2006) 483–491, https://doi.org/10.1007/s00792-006-0525-0.
[31] R. Papa, L. Selan, E. Parrilli, M. Tilotta, F. Sannino, G. Feller, M. Artini, Anti-biofilm activities from marine cold adapted Bacteria against staphylococci and *Pseudomonas aeruginosa*, Front. Microbiol. (2015), https://doi.org/10.3389/fmicb.2015.01333. Volume 6-2015.
[32] R. Papa, G. Vrenna, C. D'Angelo, A. Casillo, M. Relucenti, O. Donfrancesco, L. Selan, Anti-virulence activity of the cell-free supernatant of the Antarctic bacterium Psychrobacter sp. TAE2020 against *Pseudomonas aeruginosa* clinical isolates from cystic fibrosis patients, Antibiotics 10 (8) (2021) 944, https://doi.org/10.3390/antibiotics10080944.
[33] S. Pengfei, Y. Yifan, L. Linhui, L. Yimin, X. Dan, G. Shaowei, H. Guanqing, W. Yong, Novel antibiotics against *Staphylococcus aureus* without detectable resistance by targeting proton motive force and FtsH, MedComm 6 (1) (2020) e70046, https://doi.org/10.1002/mco2.70046.
[34] Z. Qin, Y. Ou, L. Yang, Y. Zhu, T. Tolker-Nielsen, S. Molin, D. Qu, Role of autolysin-mediated DNA release in biofilm formation of *Staphylococcus epidermidis*, Microbiology 153 (7) (2007) 2083–2092, https://doi.org/10.1099/mic.0.2007/006031-0.
[35] S. Raue, S.-H. Fan, R. Rosenstein, S. Zabel, A. Luqman, K. Nieselt, F. Götz, The genome of *Staphylococcus epidermidis* O47, Front. Microbiol. 11 (2020) 2061, https://doi.org/10.3389/fmicb.2020.02061.
[36] P. Sahariah, F. Papi, K.L. Merz, O.E. Sigurjonsson, R.L. Meyer, C. Nativi, Chitosan–saccharide conjugates for eradication of *Pseudomonas aeruginosa* biofilms, RSC Appl. Polym. 2 (3) (2024) 461–472, https://doi.org/10.1039/d3lp00263b.
[37] L. Selan, R. Papa, A. Ermocida, A. Cellini, E. Ettorre, G. Vrenna, D. Campoccia, L. Montanaro, C.R. Arciola, M. Artini, Serratiopeptidase reduces the invasion of osteoblasts by Staphylococcus aureus, Int. J. Immunopathol. Pharmacol. 30 (4) (2017) 423–428, https://doi.org/10.1177/0394632017745762.
[38] M. Tabouret, J. de Rycke, G. Dubray, Analysis of surface proteins of Listeria in relation to species, serovar and pathogenicity, J. Gen. Microbiol. 138 (4) (1992) 743–753, https://doi.org/10.1099/00221287-138-4-743.
[39] C. Vuong, M. Otto, *Staphylococcus epidermidis* infections, Microbes Infect. 4 (4) (2002) 481–489, https://doi.org/10.1016/S1286-4579(02)01563-0.
[40] F. Valour, S. Trouillet-Assant, J.P. Rasigade, S. Lustig, E. Chanard, H. Meugnier, S. Tigaud, F. Vandenesch, J. Etienne, T. Ferry, F. Laurent, Lyon BJI Study Group, Staphylococcus epidermidis in orthopedic device infections: the role of bacterial internalization in human osteoblasts and biofilm formation, PLoS One 8 (6) (2013) e67240, https://doi.org/10.1371/journal.pone.0067240.

[41] A. Wadood, M. Ghufran, A. Khan, S.S. Azam, R. Uddin, M. Waqas, S. Saleem, The methicillin-resistant *S. Epidermidis* strain RP62A genome mining for potential novel drug targets identification, Gene Rep. 8 (2017) 88–93, https://doi.org/10.1016/j.genrep.2017.06.002.

[42] J. Wang, D.D. Risola, R. Mattioli, N. Zoratto, L. Mosca, C.D. Meo, P. Matricardi, Hyaluronan-cholesterol nanogels embedding betamethasone for the treatment of skin inflammatory conditions, Int. J. Pharm. 668 (2025) 124978, https://doi.org/10.1016/j.ijpharm.2024.124978.

[43] J. Wang, M. Viola, C. Migliorini, L. Paoletti, S. Arpicco, C. Di Meo, P. Matricardi, Polysaccharide-based Nanogels to overcome mucus, skin, cornea, and blood-brain barriers: a review, Pharmaceutics 15 (10) (2023) 2508, https://doi.org/10.3390/pharmaceutics15102508.

[44] W. Xi, V. Hegde, S.D. Zoller, H.Y. Park, C.M. Hart, T. Kondo, T. Segura, Point-of-care antimicrobial coating protects orthopaedic implants from bacterial challenge, Nat. Commun. 12 (1) (2021) 5473, https://doi.org/10.1038/s41467-021-25383-z.

[45] W. Xia, J. Li, Q. Cai, C. Deng, Z. Zhou, X. Yu, C. Huang, B. Cheng, Exploring the antibiofilm potential of chitosan nanoparticles by functional modification with chloroquine and deoxyribonuclease, Carbohydr. Polym. 347 (2025) 122726, https://doi.org/10.1016/j.carbpol.2024.122726.

[46] S. Zheng, M. Bawazir, A. Dhall, H.-E. Kim, L. He, J. Heo, G. Hwang, Implication of surface properties, bacterial motility, and hydrodynamic conditions on bacterial surface sensing and their initial adhesion, Front. Bioeng. Biotechnol. 9 (2021) 643722, https://doi.org/10.3389/fbioe.2021.643722.

[47] W. Ziebuhr, S. Hennig, M. Eckart, H. Kränzler, C. Batzilla, S. Kozitskaya, Nosocomial infections by *Staphylococcus epidermidis*: how a commensal bacterium turns into a pathogen, Int. J. Antimicrob. Agents 28 (2006) 14–20, https://doi.org/10.1016/j.ijantimicag.2006.05.012.

[48] N. Zoratto, L. Forcina, R. Matassa, L. Mosca, G. Familiari, A. Musarò, P. Matricardi, Hyaluronan-cholesterol Nanogels for the enhancement of the ocular delivery of therapeutics, Pharmaceutics 13 (11) (2021) 1781, https://doi.org/10.3390/pharmaceutics13111781.